ELKHA : Jurnal Teknik Elektro, Vol. 15 No.2, October 2023, pp. 112 - 119
ISSN: 1858-1463 (print), 2580-6807 (online)

Temperature and Humidity Control System for Pole-Mounted Metering Circuit Breaker with Artificial Neural Network Methods

Mirza Ghulam Ahmad[1*)], Moh. Zaenal Efendi[2)], and Rachma Prilian Eviningsih[3)]

[1,2,3)] Department of Electrical Engineering, Politeknik Elektronika Negeri Surabaya, Indonesia
Corresponding Email: [*)] mirzaghulamahmad@pe.student.pens.ac.id

***Abstract* – Pole-mounted Metering Circuit Breaker (PMCB) is a medium voltage protection device. Problems in the PMCB because operating at medium voltage causes insulation problems. The isolation problem that arises is due to partial discharge. Partial discharge can trigger the risk of flashover. In addition, corona discharge causes corrosion of the conductor, the effect is a failure and disconnection of electricity. This control system aims to maintain the temperature and humidity of the PMCB at the nominal values according to the standard. Based on SPLN D3.021-1:2020, it is known that under normal service conditions, the ambient air temperature does not exceed 40°C and the average temperature for 24 hours does not exceed 35°C and the highest relative humidity is 100% RH. The control system uses an AC voltage controller which is used to control the input voltage of the heater and exhaust fan so that the temperature and humidity can reach nominal operating conditions. The control method used is an artificial neural network (ANN) to find the ignition angle of the AC voltage controller as a TRIAC control. The test results using the ANN control method, system simulation produces a temperature error of 1.029% and humidity error of 2.48% and the hardware system produces a temperature error of 2.364% and humidity error of 8.673% compared to the set point temperature of 35°C and humidity of 50% RH. It can be concluded that the ANN control method can maintain the PMCB temperature and humidity according to standards.**

Keywords*: *Artificial neural network, exhaust fan, heater, PMCB.

I. INTRODUCTION

Pole-mounted Metering Circuit Breaker (PMCB) is a medium voltage protection device [1]. One of the PMCB components is the Vacuum Circuit Breaker (VCB). PMCB is widely applied in densely populated areas where fire resistance and low maintenance are required [1]. Because PMCB operates on medium voltage, insulation problems arise in the PMCB equipment. Isolation problems that arise are caused by partial discharge [2]–[7]. Examples of partial discharge are internal discharge, surface discharge and coronal discharge [5]. Partial discharge can trigger the risk of flashover [4],[8],[9]. Since corona discharge causes corrosion of the conductors, the resulting effects are failure of electronic components and disconnection of the electrical connections which affect the performance and reliable operation [10]–[13].

This research aims to produce a system that can control the temperature and humidity in the PMCB always at standard nominal operating conditions to prevent these disturbances from occurring [14],[15]. Standard values based on SPLN D3.021-1:2020 are normal service conditions ambient air temperature does not exceed 40°C and the average temperature for 24 hours does not exceed 35°C and the highest relative humidity is 100% RH. This system is a new idea in the method of controlling temperature and humidity. The system adds an exhaust fan to dissipate excess heat and regulates the heater temperature on the PMCB. Exhaust fan and heater control is carried out using an AC voltage controller with the ANN control method [16].

The AC voltage controller controls the input voltage of the heater and exhaust fan so that the temperature of the heater and the speed of the exhaust fan are controlled so that the temperature and humidity of the PMCB are maintained. [17]. Based on the research that has been done, the ANN control method is used to control the AC voltage controller which works by finding the ignition angle of the AC voltage controller [16],[18]. The ANN control method modelling has complex relationships between inputs and outputs to reveal patterns in the data. ANN has been implemented in the classification field [19]. The ANN control method works by searching for the ignition angle of the AC voltage controller based on the temperature and humidity values read by the DHT22 sensor. Thus, the ANN control method will classify the temperature and humidity that are read by the DHT22 sensor to find the ignition angle of the AC voltage controller which produces an output voltage to control the heater and exhaust fan whose temperature and humidity correspond to the set point value according to the nominal operating standard. If the temperature is above the nominal standard, the heater turns off and the exhaust fan works. If the humidity is above the standard nominal, the heater works and the exhaust fan turns off. The condition is the opposite. Heaters and exhaust fans work in opposite directions. In this system, there are 4 ZMPT101B voltage sensors on each AC input and output voltage controller to

Manuscript received 2023-07-24 ; revised 2023-08-08; accepted 2023-09-13

measure voltage values. The LCD in this system serves as a display of temperature and humidity information on the PMCB which greatly helps the work of the electrical operator.

II. METHODOLOGY

Research [16], used the ANN control method to search for the optimal ignition angle of the AC voltage controller within a certain operating range. Research [18], used the ANN control method with backpropagation learning data to monitor circuit breaker temperature and humidity then the system will predict the working state and remaining service life and give an alarm for the breakdown.

Based on previous research, this research has the advantage of using research or systems that have been made before, namely the system not only monitors temperature and humidity on the PMCB, but also has actions to control temperature and humidity using a heater and exhaust fan whose input voltage is controlled using AC voltage controller whose ignition angle is classified using ANN control method. This system is also able to monitor the voltage at each input and output of the AC voltage controller and display temperature and humidity information on the LCD.

A. System Design

Figure 1 shows the block diagram of the system with the main components of the system. The main components of the system include the STM32 microcontroller, AC voltage controller, DHT22 temperature and humidity sensor, ZMPT101B voltage sensor, LCD, heater and exhaust fan. The voltage source of this system is 220 VAC.

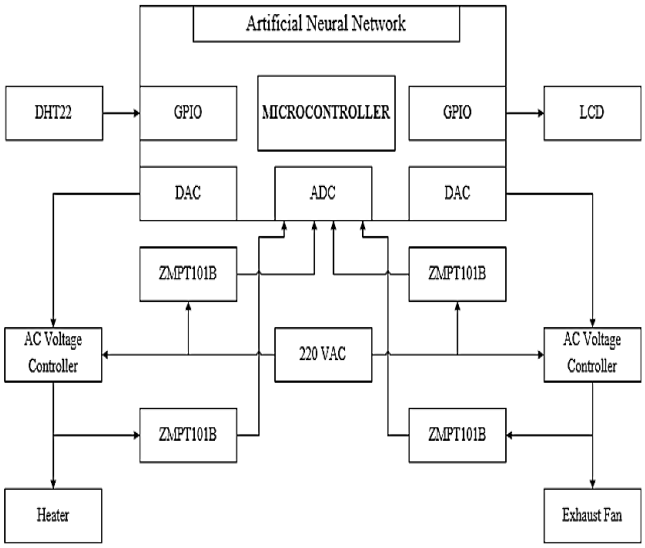

Figure 1. Block diagram system

Figure 2 shows a system flowchart that shows the workflow of the system from the start of the system to the end of the system.

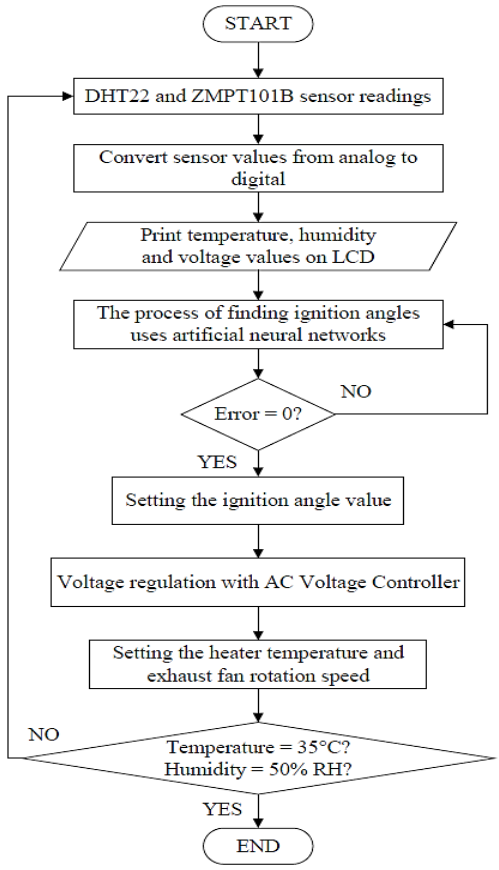

Figure 2. Flowchart system

The system flowchart starts from a reading of the DHT22 temperature and humidity sensor. There is also a reading of the ZMPT101B voltage sensor on each input and output of the AC voltage controller. The results of the DHT22 and ZMPT101B sensor readings are processed by the microcontroller. The value of the sensor reading is displayed on the LCD. The temperature and humidity values are classified using the ANN control method with a target ignition angle value for the TRIAC control on the AC voltage controller. So that an output voltage is generated to regulate the temperature of the heater and the rotational speed of the exhaust fan so that the temperature and humidity reach the set point values of 35ºC and 50% RH.

B. System Hardware Design

1). PMCB Box

Based on the PMCB manual book page 13, the PMCB switching box has dimensions of 130.5 cm long, 125 cm wide and 90 cm high. Figure 3 shows the placement of the DHT22 temperature and humidity sensor, heater and exhaust fan in the PMCB box. The reason for putting the heater on the bottom and the exhaust fan on top is because heat moves from the bottom up and the function of the exhaust fan is to dissipate excess heat in the PMCB box to control temperature [20]. The PMCB box is planned to be made of iron with a thickness of 1.5 millimetres. Because the PMCB box material is iron, and iron is a conductor that has high thermal conductivity [21].

Figure 3. Placement of the DHT22 temperature and humidity sensor, heater and exhaust fan

Figure 4 shows the placement of the control system hardware outside the PMCB box. The control system hardware consists of a microcontroller, 2 AC voltage controllers, 4 voltage sensors and an LCD.

Figure 4. Placement of control system hardware

2). Heater

The heater functions to control humidity. Based on the PMCB manual book page 12, the heater specifications used are heaters that use a voltage rating of 220–400 V with a power of 150 W and have a temperature scale of 30–110°C.

3). Exhaust Fan

The exhaust fan functions to control and remove the excess temperature. To determine the exhaust fan specifications used, it is necessary to know the CMH value. The following is the equation for calculating air circulation :

$$CMH = V \times ACH \quad (1)$$

where CMH is the air volume can be pull in one hour, V is the air volume and ACH is the air changes per hour.

C. Artificial Neural Network Design

The ANN in this system uses the multilayer network architecture type with the data feed-forward backpropagation learning method. The feed-forward backpropagation data learning method allows to solve different prediction, recognition and classification problems using smaller networks and simpler learning algorithms than those used traditionally as well as demonstrating good performance in convergence speed [22]. The architectural model of the ANN in this system uses multi-input and multi-output because there are 2 inputs and 2 outputs. 2 inputs are temperature and humidity and 2 outputs are ignition angles.

Based on references from [23]–[28], there are 3 points of the training or learning process in backpropagation neural networks. First, the forward propagation has 3 steps:

- The first step is that from the input layer there is an input unit obtained from the results of the DHT22 temperature and humidity sensor readings which are then forwarded to each neuron in hidden layer 1.
- The second step is to calculate the output value for each neuron in hidden layer 1.

$$z_{net_j} = W_{jo} + \sum_{i=1}^{n} X_i W_{ji} \quad (2)$$

$$z_j = f\left(z_{net_j}\right) = \frac{1-e^{-(z_{net_j})}}{1+e^{-(z_{net_j})}} \quad (3)$$

- The third step is to calculate the output value for each neuron in hidden layer 2.

$$z_{net_j} = V_{jo} + \sum_{i=1}^{n} X_i V_{ji} \quad (4)$$

$$z_j = f\left(z_{net_j}\right) = \frac{1}{1+e^{-(z_{net_j})}} \quad (5)$$

where z_j is the output hidden layer value, W_{jo} is the output weight hidden layer 1 value, V_{jo} is the output weight hidden layer 2 value, X_i is the input value, W_{ji} is the input weight hidden layer 1 value, V_{ji} is the input weight hidden layer 2 value and f is the activation function.

After the next forward propagation process is the back-propagation process where there are three stages as follows:

- The first step is to calculate the δ factor at the output layer based on the error value of each unit output.

$$\delta_k = (t_k - y_k) f'(y_{net_k}) \quad (6)$$

Perform calculations of the speed of change of weights in W_{kj} with α

$$\Delta W_{kj} = \alpha \delta_k Z_j \quad (7)$$

- The second step is calculating the δ factor in hidden layer 2 based on the error value of each neuron.

$$\delta_{net_j} = \sum_{j=1}^{i} \delta_i W_{ij} \quad (8)$$

Then the δ factor value in hidden layer 2,

$$\delta_j = \delta_{net_j} f'(z_{net_j}) \quad (9)$$

- The third step is calculating the δ factor in hidden layer 1 based on the error value of each neuron.

$$\delta_{net_j} = \sum_{j=1}^{i} \delta_i Y_{ij} \quad (10)$$

Then the δ factor value in hidden layer 1,

$$\delta_j = \delta_{net_j} f'(W_{net_j}) \quad (11)$$

where δ_k is the gradient error in the output layer, t_k is the

actual target, y_k is the actual output at the output layer, y_j is the actual output at the hidden layer α is the acceleration rate and δ_j is the gradient error in the hidden layer.

And in the last process, namely determining the weight changes in the back propagation ANN algorithm:

- Change of weights in hidden layer 1

$$W_{ij(new)} = W_{ij(old)} + \Delta W_{ij} \quad (12)$$

- Changes in weights on the hidden layer 2

$$V_{ij(new)} = V_{ij(old)} + \Delta V_{ij} \quad (13)$$

- Changes in weights on the output layer

$$Z_{ij(new)} = Z_{ij(old)} + \Delta V_{ij} \quad (14)$$

where $W_{ij(new)}$ is the new input weight hidden layer 1 value, $W_{ij(old)}$ is the old input weight hidden layer 1 value, ΔW_{ij} is the change of weights in hidden layer 1, $V_{ij(new)}$ is the new input weight hidden layer 2 value, $V_{ij(old)}$ is the old input weight hidden layer 2 value, ΔV_{ij} is the change of weights in hidden layer 2, $Z_{ij(new)}$ is the new input weight output layer and $Z_{ij(old)}$ is the old input weight output layer.

D. System Simulation Design

System simulation design includes AC voltage controller and ANN control method. System simulation to prove that the planned hardware system works and the data is used as a comparison with hardware data.

The following is the theoretical calculation equation for the output voltage of the AC voltage controller [29]–[32].

$$V_{o(RMS)} = \frac{V_m}{\sqrt{2}}\sqrt{1 - \frac{\alpha}{\pi} + \frac{\sin(2\alpha)}{2\pi}} \quad (15)$$

where $V_{o\ (RMS)}$ is the output RMS voltage, V_m is the maximum voltage and α is the ignition angle.

Based on Figure 5 is a system simulation circuit with a temperature set point of 35°C and 50% RH humidity. This simulation is done using Matlab software.

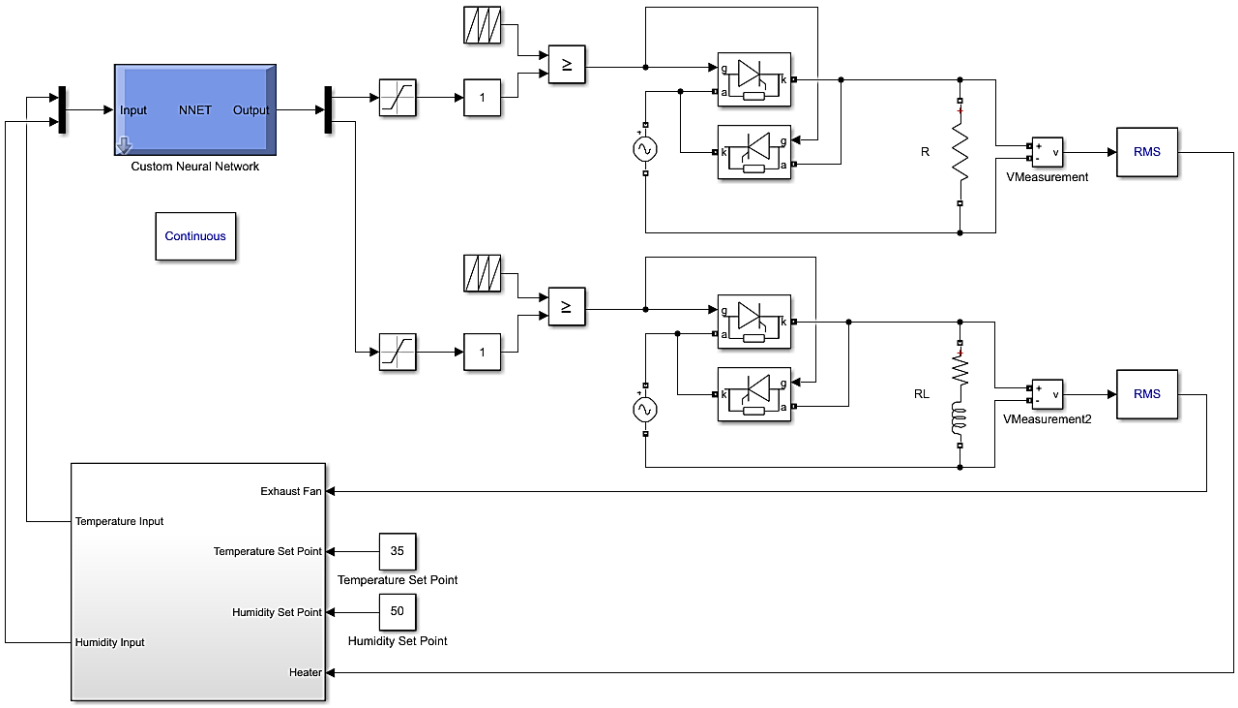

Figure 5. System simulation circuit

Based on Figure 5, the system needs a transfer function as a representation of the temperature and humidity response system. Based on Modern Control Engineering by Katsuhiko Ogata, the transfer function value is used to convert the voltage value into a temperature response output in a system simulation. From a mathematical model of a system, the order of a system can be seen from the power of the variable s (in the Laplace transform). A system is said to be first-order if its transfer function has a variable s with the highest power of one. The first order system model can be written mathematically as follows:

$$\frac{C(s)}{R(s)} = \frac{K}{\tau_s + 1} \quad (16)$$

To determine the parameter K (gain overall) if the system is linear, then the relationship Y_{ss} with X_{ss} can be written as follows:

$$K = \frac{Y_{ss}}{X_{ss}} \quad (17)$$

The analytical formula for calculating the response parameters of the first order is as follows:

Steady time (0,5%)

$$t_s = 5\tau \quad (18)$$

where $C(s)$ is the system output, $R(s)$ is the system input, K is the overall gain, $\tau_s + 1$ is the time reaches 63.2% (seconds) in first order, Y_{ss} is the set point, X_{ss} is the response results and t_s is the steady time.

The transfer function value of the calculation results will be entered in the block on the Matlab Simulink software.

III. Results and Discussion

Table 1 shows the results of hardware testing without using the ANN control method. The test was carried out in the afternoon for 30 minutes.

Table 1. Hardware Test Results Without ANN

Time (Minute)	Temperature Set Point (°C)	Temperature (°C)	Humidity Set Point (%RH)	Humidity (%RH)
0	35	30	50	64.3
3	35	33.2	50	58
6	35	35.7	50	52.6
9	35	39	50	47
12	35	42.8	50	41.3
15	35	45.6	50	37.6
18	35	49	50	34.4
21	35	51.1	50	32.4
24	35	53.3	50	30.4
27	35	54.5	50	27.8
30	35	55.3	50	25

Based on Table 1 it is known that the temperature value at the initial test conditions is 30°C and the humidity is 64.3% RH. In steady state conditions, the temperature is 55.3°C and the humidity is 25%RH. The temperature value reaches the set point of 35°C within 6 minutes with an average error of 27.143%, while the humidity value reaches the set point of 50%RH within 9 minutes with an average error of 18.036%. Based on the data from hardware testing without the ANN control method, it can be concluded that the system can be controlled because it is able to achieve the planned set point value and ANN control methods can be added.

Figure 6 and Figure 7 are graphs comparing the output response of temperature and humidity to the time of the simulation test results without using the ANN and using the ANN control method using the Matlab software.

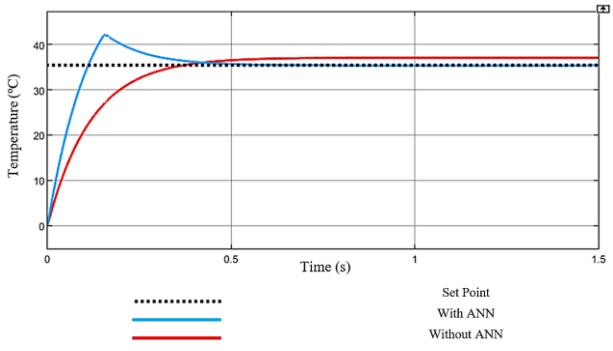

Figure 6. Comparison graph of the temperature simulation test results without using the ANN and using the ANN control method

Based on Figure 6, it is known that the output response of the system using the ANN control method is steady state at the set point temperature conditions, while the output response of the system without using the ANN control method is steady state at conditions of temperatures exceeding the set point. Based on Figure 6, it can be seen that the response time parameters are shown in Table 2.

Table 2. Time Response of Graph of the Temperature Simulation Test Results

Time Response	Without ANN	With ANN
Rise time (ms)	252.003	84.391
Overshoot (%)	0.995	20.122
Steady state error (%)	6	1.029

Based on Table 2, it is known that the rise time of the system using the ANN control method is smaller which indicates the system is able to approach the set point value more quickly. However, the fast rise time results in an overshoot value that is 20 times greater than without using the ANN control method. In steady state conditions, the system without using the ANN steady state control method is at 37.1°C with an error of 6%, while the system uses the ANN steady state control method at 35.36°C with an error of 1.029%.

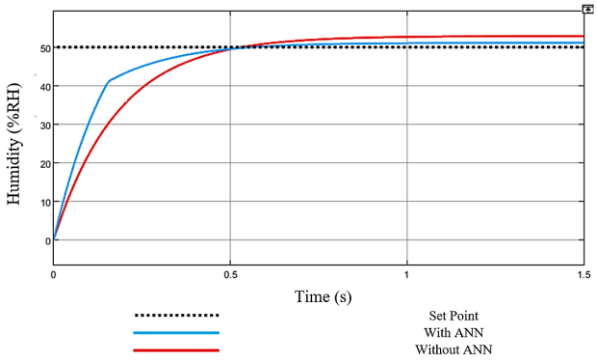

Figure 7. Comparison graph of the humidity simulation test results without using the ANN and using the ANN control method

Based on Figure 7, it is known that the output response of the system using the ANN control method is steady state at the set point humidity conditions, while the output response of the system without using the ANN control method is steady state at conditions of humidity exceeding the set point. Based on Figure 7, it can be seen that the response time parameters are shown in Table 3.

Table 3. Time Response of Graph of the Humidity Simulation Test Results

Time Response	Without ANN	With ANN
Rise time (ms)	388.237	265.3
Overshoot (%)	0.872	0.41
Steady state error (%)	6	2.48

Based on Table 3, it is known that the rise time of the system using the ANN control method is smaller which indicates the system is able to approach the set point value more quickly. However, the fast rise time results in a smaller overshoot value than without using the ANN control method. In steady state conditions, the system without using the ANN steady state control method is at 53%RH with an error of 6%, while the system uses the ANN steady state control method at 51.24%RH with an error of 2.48%.

Based on the results of system simulation testing without using the ANN and using the ANN control method at temperature and humidity, it is known that using the ANN control method produces a smaller steady state error value which indicates the results are closer to the set point.

After getting the results of system simulation testing with small error results, the ANN control method can be tested on hardware testing. System hardware testing using the ANN control method was carried out at night for 30 minutes. The results of system hardware testing with the ANN control method are shown in Table 4.

Table 4. Hardware Test Results with ANN

Time (Minute)	Temperature Set Point (°C)	Temperature (°C)	Humidity Set Point (%RH)	Humidity (%RH)
0	35	28.9	50	73.9
3	35	37.1	50	53.4
6	35	36.6	50	52.8
9	35	36.9	50	52.3
12	35	36	50	53.7
15	35	37	50	52.2
18	35	36.1	50	52.2
21	35	35.8	50	52.9
24	35	37.5	50	50.2
27	35	36.4	50	51.2
30	35	35.8	50	52.9

Based on Table 4, it can be seen the graph of temperature against time and humidity against time in Figure 8 and Figure 9.

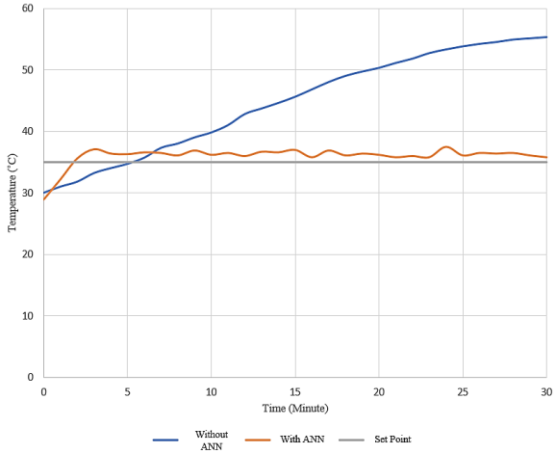

Figure 8. Graph of characteristics of temperature against time

Based on Figure 8, it is known that the response of the output temperature to the time the system hardware test results without the ANN control method is unable to maintain the temperature at the set point value because the temperature value will continue to rise until it reaches a steady state value according to the temperature that can be produced by a heater with a power of 150 W The results of system hardware testing using the ANN control method were able to maintain temperatures around the set point value of 35 °C. The average error of system hardware testing without using the ANN control method in steady state conditions is 27.143%. After adding the ANN control method, the average error in system hardware testing at steady state conditions is 2.364%.

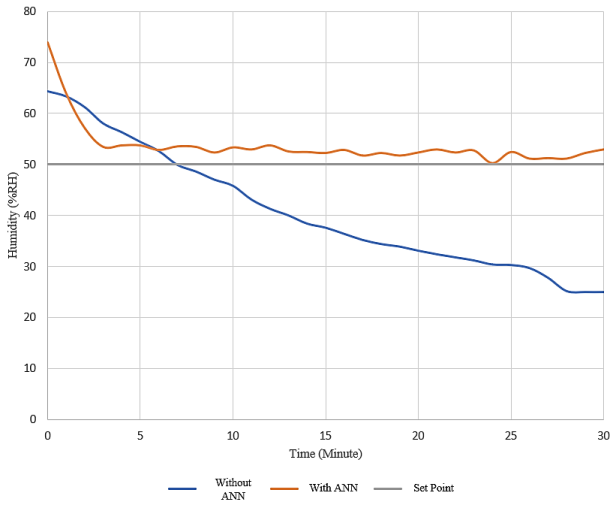

Figure 9. Graph of characteristics of humidity against time

Based on Figure 9, it is known that the response of output humidity to the time of system hardware test results without the ANN control method is not able to maintain the temperature at the set point value because the humidity value will continue to rise until it reaches a steady state value according to the humidity that can be produced by a heater with a power of 150 W The results of system hardware testing using the ANN control method were able to maintain temperatures around the set point value of 50%RH. The average error of system hardware testing without using the ANN control method in steady state conditions is 18.036%. After adding the ANN control method, the average error in system hardware testing at steady state conditions is 8.673%.

The results of the addition of the ANN control method to the system simulation and system hardware show the average error results shown in Table 5. The average error is the result of a comparison between the temperature and humidity values of the test results compared to the setpoint value.

Table 5. Comparison of System Test Error Values Using the ANN Control Method

Parameter	Set Point	Simulation error	Hardware error
Temperature	35°C	1.029%	2.364%
Humidity	50%RH	2.48%	8.673%

Based on Table 5, it is known that the average temperature error in the system simulation test results compared to hardware testing using the ANN control method shows an identical value with a small average error. However, the average error of humidity in the system simulation test results compared to hardware testing using the ANN control method shows that there is a difference in value but is still categorized as a small average error.

Errors in temperature and humidity in the system hardware test results are caused by weather factors (temperature and humidity) at the test location and heat conductivity. Because the PMCB box material is iron and iron is a conductor so it has a high thermal conductivity.

So this affects the temperature and humidity in the PMCB box because if the temperature somewhere is high then the humidity is low and the opposite if the temperature is low then the humidity is high.

In addition, based on Figure 6, Figure 7, Figure 8 and Figure 9, it can be seen that by adding the ANN control method it is able to reduce the error value to be smaller when compared to not using the ANN control method. This shows that the ANN control method is able to maintain the temperature and humidity values at the standard nominal or set point value.

IV. Conclusion

Based on the results of testing the temperature and humidity control system on the PMCB using a heater and exhaust fan with the ANN control method, it can be seen that the advantage of adding the ANN control method can reduce errors and obtain stable values around the set point. The results of system testing without using the ANN control method in the simulation produce a temperature error of 6% and a humidity error of 6% and the hardware produces a temperature error of 27.143% and a humidity error of 18.036% compared to the set point value. However, after adding the ANN control method to the system, the simulation produces a temperature error of 1.029% and a humidity error of 2.48% and the hardware produces a temperature error of 2.364% and a humidity error of 8.673% compared to the set point value. It can be concluded that by adding the ANN control method can reduce the error value and produce an output value close to the set point. For future research, it is recommended to conduct a disturbance test to determine the performance of the control method and use a different control method as a comparison.

Acknowledgement

The author would like to thank the supervisors who have guided the research and the Politeknik Elektronika Negeri Surabaya for facilitating the research.

References

[1] M. Homma, M. Sakaki, E. Kaneko, and S. Yanabu, ‘History of vacuum circuit breakers and recent developments in Japan’, *IEEE Trans. Dielectr. Electr. Insul.*, vol. 13, no. 1, pp. 85–92, 2006.

[2] M. A. Douar, A. Beroual, and X. Souche, ‘Assessment of the resistance to tracking of polymers in clean and salt fogs due to flashover arcs and partial discharges degrading conditions on one insulator model’, *IET Gener. Transm. Distrib.*, vol. 10, no. 4, pp. 986–994, Mar. 2016.

[3] C. Sitompul, Z. Nawawi, and M. I. Jambak, ‘Detection of Polymer Insulator Surface Based on the Effects of Tropical Climate Using Partial Discharge Signals Measurement’, *J. Phys. Conf. Ser.*, vol. 1500, p. 12019, Apr. 2020.

[4] S. Chandrasekar, C. Kalaivanan, G. C. Montanari, and A. Cavallini, ‘Partial discharge detection as a tool to infer pollution severity of polymeric insulators’, *IEEE Trans. Dielectr. Electr. Insul.*, vol. 17, no. 1, pp. 181–188, 2010.

[5] V. Padma and V. S. Raghavan, ‘Analysis of insulation degradation in Insulators using Partial Discharge analysis’, in *2011 3rd International Conference on Electronics Computer Technology*, 2011, pp. 110–114.

[6] Y. Liu *et al.*, ‘Corona onset gradient of the bundle conductor on AC power lines under sand and dust weather condition at 2,200 m altitude’, *J. Electrostat.*, vol. 95, pp. 32–41, 2018

[7] L. Yunpeng *et al.*, ‘Corona loss of the bundle conductors on EHV/UHV AC power lines under sandy and dusty conditions in high-altitude areas’, *J. Electrostat.*, vol. 107, p. 103476, 2020.

[8] K. Takabayashi, R. Nakane, H. Okubo, and K. Kato, ‘High voltage DC partial discharge and flashover characteristics with surface charging on solid insulators in air’, *IEEE Electr. Insul. Mag.*, vol. 34, no. 5, pp. 18–26, 2018.

[9] Q. Xiong, L. Zhu, S. Ji, Y. Cui, and W. Lu, ‘Flashover and partial discharge characteristics of fiber of valve tower in converter station’, *IEEE Trans. Dielectr. Electr. Insul.*, vol. 24, no. 4, pp. 1985–1991, 2017.

[10] N. A. Salim, J. Jasni, and M. M. Othman, ‘Reliability assessment by sensitivity analysis due to electrical power sequential tripping for energy sustainability’, *Int. J. Electr. Power Energy Syst.*, vol. 126, p. 106582, 2021.

[11] J.-R. Riba, J. Martínez, M. Moreno-Eguilaz, and F. Capelli, ‘Characterizing the temperature dependence of the contact resistance in substation connectors’, *Sensors Actuators A Phys.*, vol. 327, p. 112732, 2021.

[12] T. Wu, Z. Zhou, S. Xu, Y. Xie, L. Huang, and F. Yin, ‘A corrosion failure analysis of copper wires used in outdoor terminal boxes in substation’, *Eng. Fail. Anal.*, vol. 98, pp. 83–94, 2019.

[13] A. Fateh, M. Aliofkhazraei, and A. R. Rezvanian, ‘Review of corrosive environments for copper and its corrosion inhibitors’, *Arab. J. Chem.*, vol. 13, no. 1, pp. 481–544, 2020.

[14] P. Wang, J. Sun, P. Zhang, J. Wang, and Z. Zhao, ‘Numerical simulation of the condensation process in high voltage switchgear based on the temperature and humidity distribution’, *J. Phys. Conf. Ser.*, vol. 2087, no. 1, p. 12082, 2021.

[15] D. Song, Y. Cao, and H. Xu, ‘Reduce the factor of space humidity on the incorrect action of circuit breakers’, in *2011 International Conference on Advanced Power System Automation and Protection*, 2011, pp. 93–96.

[16] S. Kaitwanidvilai and P. Piyarungsan, ‘Low-cost microprocessor-based alternating current voltage controller using genetic algorithms and neural network’, *IET Power Electron.*, vol. 3, no. 4, pp. 490–499, 2010.

[17] J. Monicka, D. Sekhar, and K. Kumar, ‘Performance Evaluation of Membership Functions on Fuzzy Logic Controlled AC Voltage Controller for Speed Control of Induction Motor Drive’, *Int. J. Comput. Appl.*, vol. 13, Jan. 2010.

[18] Y. Hou, T. Liu, X. Lun, J. Lan, and Y. Cui, ‘Research on Monitoring System of Circuit Breakers Based on Neural Networks’, in *2010 International Conference on Machine Vision and Human-machine Interface*, 2010, pp. 436–439.

[19] M. Al-Shawwa, A. Al-Absi, S. Hassanein, K. Baraka, and S. Abu-Naser, 'Predicting Temperature and Humidity in the Surrounding Environment Using Artificial Neural Network', *Int. J. Acad. Dev.*, vol. 2, pp. 1–6, Sep. 2018.

[20] Y. Behjat, S. Shahhosseini, and S. H. Hashemabadi, 'CFD modeling of hydrodynamic and heat transfer in fluidized bed reactors', *Int. Commun. Heat Mass Transf.*, vol. 35, no. 3, pp. 357–368, 2008.

[21] E. S. Toberer, L. L. Baranowski, and C. Dames, 'Advances in Thermal Conductivity', *Annu. Rev. Mater. Res.*, vol. 42, no. 1, pp. 179–209, Jul. 2012.

[22] I. Aizenberg and C. Moraga, 'Multilayer Feedforward Neural Network Based on Multi-valued Neurons (MLMVN) and a Backpropagation Learning Algorithm', *Soft Comput.*, vol. 11, no. 2, pp. 169–183, 2007.

[23] I. Aizenberg *et al.*, 'A multi-step approach to the single fault diagnosis of DC-DC switched power converters', in *2018 IEEE International Symposium on Circuits and Systems (ISCAS)*, 2018, pp. 1–5.

[24] M. A. Abdulrachman, E. Prasetyono, D. O. Anggriawan, and A. Tjahjono, 'Smart Detection Of AC Series Arc Fault On Home Voltage Line Based On Fast Fourier Transform And Artificial Neural Network', in *2019 International Electronics Symposium (IES)*, 2019, pp. 439–445.

[25] I. Aizenberg, D. V Paliy, J. M. Zurada, and J. T. Astola, 'Blur Identification by Multilayer Neural Network Based on Multivalued Neurons', *IEEE Trans. Neural Networks*, vol. 19, no. 5, pp. 883–898, 2008.

[26] A. F. Mubarok, T. Octavira, I. Sudiharto, E. Wahjono, and D. O. Anggriawan, 'Identification of harmonic loads using fast fourier transform and radial basis Function Neural Network', in *2017 International Electronics Symposium on Engineering Technology and Applications (IES-ETA)*, 2017, pp. 198–202.

[27] I. Sudiharto, O. Dimas, Anggriawan, and A. Tjahjono, 'Harmonic Load Identification Based On Fast Fourier Transform And Levenberg Marquardt Backpropagation', *J. Theor. Appl. Inf. Technol.*, vol. 95, Apr. 2017.

[28] O. Keohane and I. Aizenberg, 'Impulse Noise Filtering using MLMVN', in *2020 International Joint Conference on Neural Networks (IJCNN)*, 2020, pp. 1–8.

[29] A. A. Rachman, Y. C. Arif, and L. P. S. Raharja, 'Inrush Current Limiter in 3-Phase Transformer Using AC Voltage Controller Simulation Using SIMULINK®', in *2020 International Conference on Technology and Policy in Energy and Electric Power (ICT-PEP)*, 2020, pp. 156–161.

[30] L. Siang Tat and Y. Kah Haur, 'Remote AC Power Control by Using Microcontroller', *J. Telecommun. Electron. Comput. Eng.*, vol. 8, no. 12 SE-Articles, pp. 53–58, Dec. 2016,

[31] Y. C. Arif, R. Rakhmawati, A. Saksana, and Suhariningsih, 'Implementation of AC-AC Voltage Controller for Reduce Transient Current at Three Phase Induction Motor', in *2019 International Seminar on Application for Technology of Information and Communication (iSemantic)*, 2019, pp. 465–470.

[32] S. Waghare, D. R. Tutakne, A. Deshmukh, and M. Mardikar, 'PWM controlled high power factor single phase Fan regulator', in *2019 3rd International conference on Electronics, Communication and Aerospace Technology (ICECA)*, 2019, pp. 59–64.